PERGAMON

Neuromuscular Disorders 17 (2007) 639–650

www.elsevier.com/locate/nmd

Upregulation of the creatine synthetic pathway in skeletal muscles of mature *mdx* mice

Warren C. McClure [a], Rick E. Rabon [a], Hirofumi Ogawa [b], Brian S. Tseng [a,*]

[a] *Departments of Pediatrics, Neurology and Cell & Developmental Biology University of Colorado Denver Health Science Center, The Children's Hospital Fitzsimons Campus, Mail Stop 8108, PO Box 6511, Aurora CO 80045, USA*

[b] *Department of Biochemistry, Toyama Medical and Pharmaceutical University, Faculty of Medicine, 2630 Sugitani Toyama 930-0194, Japan*

Received 30 July 2006; received in revised form 23 March 2007; accepted 2 April 2007

Abstract

Duchenne muscular dystrophy (DMD) is a fatal neuromuscular human disease caused by dystrophin deficiency. The *mdx* mouse lacks dystrophin protein, yet does not exhibit the debilitating DMD phenotype. Investigating compensatory mechanisms in the *mdx* mouse may shed new insights into modifying DMD pathogenesis. This study targets two metabolic genes, guanidinoacetate methyltransferase (GAMT) and arginine:glycine amidinotransferase (AGAT) which are required for creatine synthesis. We show that GAMT and AGAT mRNA are up-regulated 5.4- and 1.9-fold respectively in adult *mdx* muscle compared to C57. In addition, GAMT protein expression is up-regulated at least 2.5-fold in five different muscles of *mdx* vs. control. Furthermore, we find GAMT immunoreactivity in up to 80% of mature *mdx* muscle fibers in addition to small regenerating fibers and rare revertants; while GAMT immunoreactivity is equal to background levels in all muscle fibers of mature C57 mice. The up-regulation of the creatine synthetic pathway may help maintain muscle creatine levels and limit cellular energy failure in leaky *mdx* skeletal muscles. These results may help better understand the mild phenotype of the *mdx* mouse and may offer new treatment horizons for DMD. Published by Elsevier B.V.

Keywords: *mdx*; Duchenne muscular dystrophy (DMD); Creatine; Skeletal muscle; Guanidinoacetate methyltransferase (GAMT); Arginine:glycine amidinotransferase (AGAT)

1. Introduction

Duchenne Muscular Dystrophy (DMD) is the most common, severe and lethal progressive muscular dystrophy to affect children. It is also the most common inherited lethal defect worldwide (1/3500 liveborn males) [1]. There are a number of animal models of DMD including dog, cat, and mouse [2–4]; which all display varying degrees of histopathologic muscle features consistent with muscular dystrophy. The *mdx* mouse has been a valuable animal model of DMD because it lacks dystrophin protein [1], has elevated serum creatine kinase (CK) and elevated intracellular calcium [5,6] which are all similar to that of human DMD. In addition, *mdx* skeletal muscle has abnormal contractile properties [7,8] and exhibits pathologic dystrophic features [9,10] particularly in the diaphragm [11].

Despite the histopathologic similarities between the *mdx* and humans with DMD, we postulate the *mdx* mouse has made unique compensatory adaptations to dystrophin-deficiency to enable a relatively benign phenotype. The *mdx* mice exhibit cage activity indistinguishable from control mice [12], live a near normal life span [13] and can run in voluntary wheels at distances near those run by age matched control mice [13–16]. In spite of the histopathology seen in the

* Corresponding author. Address: Harvard Mass Gen Hospital, Dept of Neurology, Charlestown Naval Yard B-114, Room 2600, 16th St., Charlestown, MA 02129, USA. Tel.: +1 303 861 6895; fax: +1 617 643 0141.

E-mail address: briantseng@partners.org (B.S. Tseng).

0960-8966/$ - see front matter Published by Elsevier B.V.
doi:10.1016/j.nmd.2007.04.008

diaphragm at 6 months of age [16], *mdx* mice do not suffer respiratory failure at that age and can still exercise at levels equivalent to the levels of control mice even up to 11 months of age [13,15].

The question of how the *mdx* mouse achieves this relatively benign functional phenotype is extremely important, when considering the severe phenotype displayed in human DMD where the same protein, dystrophin, is absent. Some explanations for the phenotypic variations in species such as differences in gait and life-span are readily apparent. It seems likely that there are many other compensatory molecular mechanisms contributing in combination. Since the *mdx* mouse is not severely crippled [12], has less fibrosis and more central nuclei than human DMD [10,17,18], we postulated that there may be additional compensatory molecular pathways or modifier genes in the *mdx* mouse that warrant further investigation. Disease-modifying factors implicated in the *mdx* mouse have been described [19], such as extra-cellular matrix alterations [20–23], naturally occurring and experimental up-regulation of utrophin [24–27], myostatin inhibition [28,29], calcium protein-handling protein(s) [30–32] and enhanced satellite cell function and regeneration [33–37]. While some of these modifiers are likely important in making the *mdx* phenotype relatively benign, many of these same *mdx* changes are occurring in parallel with DMD [2,12,38,39] and cannot fully account for the clear discordant phenotypic severity. Our overarching hypothesis is that there are compensatory pathways activated via modifier genes expressed in the *mdx* mouse that are not activated in the boys with DMD.

Several large-scale expression profiling or microarray studies of the mature *mdx* mouse hind-limb muscles have been published [23,40–43]. These studies were reviewed in an effort to find the most reproducible gene expression differences and then compare to three human DMD studies [44–46]. A gene whose mRNA expression moved in parallel or the same direction (up or down) in both *mdx* mouse and human DMD were eliminated leaving only the genes that were differentially expressed (manuscript in preparation). Of these genes, two in the same metabolic pathway guanidinoacetate methyltransferase (GAMT) and arginine:glycine amidinotransferase (AGAT) were found in multiple microarray studies to be up-regulated in *mdx* vs control mice while both were down-regulated in DMD (vs human control). In mammals, GAMT and AGAT are the only two enzymes required for creatine synthesis [47,48]. We were further intrigued by this novel finding given a prior study reported upregulated creatine kinase (CK) adaptations [49]. We were struck with magnetic resonance spectroscopy (MRS) studies that showed near normal intramuscular creatine levels in *mdx* mice [50], yet intramuscular creatine levels in boys with DMD were 20% of control boys [51]. This present study reports both GAMT and AGAT upregulation for *de novo* creatine synthesis in mature *mdx* muscle, which may help limit the cellular energy failure associated with the absence of dystrophin.

2. Materials and methods

2.1. Animals, care, specimen collection and preparation

Adult control (C57BL/10ScSn) ($n = 10$) and *mdx* (C57BL/10ScSn-mdx) mice were obtained from Jackson Laboratories (Bar Harbor, ME). All mice were housed and handled in accordance with guidelines and procedures approved by Institutional Animal Care and Use Committee. Prior to being euthanized, 16 week mature mice and young mice postnatal 2 weeks, 4 weeks and 5 weeks of age were given intraperitoneal (IP) injections of pentobarbital sodium solution (100 mg/kg).

C57 ($n = 10$) and *mdx* ($n = 12$) mice age-matched at 9–11 weeks were housed with $4\frac{1}{2}$ inch running wheels (Super Pet Mini Run-Around) adapted with bicycle odometers (Sigma Sport BC 401). Weekly running distances and weights were recorded over a six-week period. Average daily running distances were determined for each mouse. These values were averaged for *mdx* and control mice for an overall value. Statistical differences between means were analyzed using Student's *t*-test.

Blood was collected via retro-orbital eye bleed. Muscle and liver specimens were excised and frozen in liquid nitrogen for homogenization. Contralateral muscles were removed, mounted in Tissue-Tek O.C.T. compound (Miles Lab, Elkhart, IN) and frozen in isopentane cooled to −160 °C in liquid nitrogen. Eight micron tissue cross-sections were obtained with a Microm cryostat at −22 °C. C57 and *mdx* tissue sections were collected onto Superfrost Plus Gold slides from Fischer Scientific and stained with H&E. Serial sections were used for immunolabelling studies (see below) and succinate dehydrogenase (SDH) histochemical stain as reported [52].

2.2. mRNA analysis

Total RNA was acid/phenol extracted from age 14–16 week old male control and *mdx* gastrocnemious mouse muscle using Trizol Reagent (Invitrogen). The RNA concentrations and purity from each sample were determined (Beckman DU 640 Spectrophotometer). Oligos (dT12–18) were used to synthesize cDNA from equal concentrations of RNA using SuperScript III Rnase H-Reverse Transcriptase (Invitrogen). Real time quantitative PCR was performed using Taq-Man reagents and ABI 7000 Prism Sequence Detection System. PCR Applied Biosystems Inc. (#377215) commercially available GAMT primers and probes, and

custom AGAT (GenBank Accession No. NC000068) primer/probe sets (Biosearch Technologies Inc.) [(FWD primer: 5′d(ATGGCTGACGAACTGTATG)3′; REV primer: 5′d(GGCCAATTTGTGTCTGT)3′ PROBE: 5′ CAL Fluor Orange 560 d(CCAGAATTATCCCATCCA TTCCGTGGA); BHQ-1 3′)] were designed to span known introns to detect contaminant genomic DNA template if present. Commercially available primers for (#386832) glyceraldehyde 3-phosphate dehydrogenase (GAPDH) (Applied Biosystems Inc.) served as an internal expression standard [53]. 96 well plates were set up with serial dilutions (1:1, 1:10, 1:100, 1:1000) of pooled control and *mdx* mouse cDNA to establish a standard curve for each primer set. Mean quantities were calculated on individual samples of control and *mdx* cDNA at 1:5 dilutions. Each PCR reaction sample was run in triplicate, and non-template controls were utilized for each primer/probe set. GAPDH, GAMT and AGAT primer pairs amplified the same cDNA stocks to determine mean fold change between control and *mdx* mouse strains and compare relative expression levels of GAMT and AGAT.

2.3. Western blot analysis

Excised muscles and liver were crushed with a mortar and pestle chilled with liquid nitrogen. Crushed tissue (100 mg/ml) was homogenized on ice for 15 s using a Fisher Power Gen 125 polytron set on 3/4 speed in buffer consisting of 1% Triton X-100, 1% sodium deoxycholate in phosphate buffered saline (PBS) with protease inhibitor cocktail (Roche). Protein concentration was determined using the BioRad DC Protein Assay Kit. Muscle (200 μg) homogenates were spun for 1 min at 7200 g. Pellets were suspended in equal volumes of ddH_2O and loading buffer then run in 12% SDS PAGE gels before transfer to nitrocellulose for immunoblotting. Liver (60 μg) homogenates served as a positive tissue control for GAMT protein. Membranes were incubated in blocking buffer containing 5% nonfat dry milk in tris-buffered saline with 0.1% Tween 20 (TTBS) at room temperature. Affinity purified rabbit anti-pig GAMT polyclonal antibodies previously used in mouse tissues (1:500 dilution) were incubated for 3 h at room temperature [54]. Protein A conjugated to HRP (Zymed) was used at a 1:1500 dilution in blocking buffer for secondary detection in ECL western blotting solution (Pierce). Blots were exposed to CL-X Posure Film (Pierce). As an internal expression control, rabbit anti-desmin polyclonal antibody 1:500 dilution was applied in blocking buffer (MP Biomedicals, #681221) and secondary detection was carried with donkey anti-rabbit Alexa-594 (Molecular Probes). Images were collected using the Typhoon 9400 imaging system and quantitation of images was done using ImageQuant (GE Healthcare).

2.4. Creatine concentration

A ninhydrin based biochemical assay was performed as published [55]. For muscle homogenates, 0.2 μg of total protein (Bio-Rad DC Kit) were used for each muscle in each reaction. For serum samples, 20 μl of each serum sample was used per reaction. Reactions were run for 10 min in black 96 well plates then fluorescence was measured using a Spectromax Fluorimeter (Molecular Devices). Concentrations were determined based on standard curves with serial dilutions using purified creatine (Sigma–Aldrich). Standard deviations were calculated and Student's *t*-tests compared values of control and *mdx*.

2.5. Indirect immunofluorescence

Ten micrometer frozen sections were stained with Hematoxylin and Eosin (H&E) while immunofluorescence used cryosections blocked with buffer consisting of 10% goat serum 0.2% Triton-X 100 in PBS. AGAT antibodies are not currently available. Affinity-purified rabbit anti-pig GAMT polyclonal antibody diluted 1:200 in blocking buffer was applied to cryosections for 4 h at room temperature [54]. As a control for non-specific binding, anti-Green Fluorescent Protein (GFP) antibody (Sigma G1544) diluted 1:100 was applied for 4 h at room temperature. Secondary antibody (donkey anti-rabbit Alexa-488; Molecular Probes) diluted 1:400 was applied to sections for 1 h. To identify early regenerating fibers, embryonic myosin heavy chain antibody (EMyHC) F1.652 (DSHB University of Iowa) diluted 1:400 [56] was secondarily labelled with secondary donkey anti-rabbit Alexa 596 (Molecular Probes). Immunofluorescence protocol was carried out using the M.O.M. kit (BMK-2202 Vector Labs) with a 1:20 primary antibody dilution and a 1:400 dilution of streptavidin Alexafluor 488 (S11223) from Molecular probes. DNA of nuclei were counterstained with 0.1% Hoechst (Sigma H6024). Sections were coverslipped with anti-fade mounting media. Images were captured on a Leica SM4000B fluorescent microscope with a Retiga 4000R QImaging CCD Camera (North Central Instruments, Inc.).

GAMT staining intensity, cell counts and cell area determination were carried out by outlining individual cell perimeters then using NIH Image software for analysis.

2.6. Evan blue vital dye

Evans Blue Dye (EBD) is a vital dye that binds to serum albumin and is excluded from the intracellular space in healthy muscle fibers. EBD penetrates fibers with membrane disruptions and can be readily visualized under fluorescence [57]. Sixteen week old C57 and *mdx* mice were given an IP injection of 2% solution EBD

(50 μl/10 g body weight) dissolved in normal saline, 4 h prior to euthanasia [57]. EBD in sections is visualized using excitation/emission (~590 nm/617 nm) filters.

3. Results

3.1. Voluntary wheel running distances

Based on previous reports, *mdx* mice run distances nearly as well as control mice in voluntary exercise wheels [13–16]. In our Colorado facility at mild altitude (5280 feet above sea level), no significant difference in running distance was observed over a six week period in mature 10–15 week old C57 ($n = 10$) and *mdx* mice ($n = 12$) (Fig. 1a). While there is some individual variation from week to week, overall C57 mice averaged 5.7 km/24 h while *mdx* averaged 5.2 km/24 h (Fig. 1b). These summary values are consistent with previous reported distances run by C57 and *mdx* mice [13–16].

3.2. mRNA analysis

To validate mRNA-based microarray and bioinformatics screening results of up-regulated GAMT and AGAT in *mdx* vs. control, Real-Time quantitative PCR was performed on mRNA from gastrocnemius muscles of *mdx* vs. control adult mice. Fig. 2 shows that GAMT RT-PCR products are 5.4-fold higher in *mdx* vs. C57 ($p = 0.003$) and AGAT RT-PCR products in *mdx* mice are 1.9-fold higher vs. control ($p = 0.047$). GAPDH served as internal expression control as previously reported [53]. This quantitative mRNA based assay demonstrates that both GAMT and AGAT mRNA expression, are upregulated in *mdx* mice vs. C57 relative to GAPDH levels.

3.3. Western blots

After verifying GAMT mRNA upregulation in gastrocnemius muscles of 16 week old *mdx* mice, GAMT immunoblots were performed on *mdx* and C57 homogenates of five different skeletal muscles. GAMT protein has a calculated MW = 26 kDa and liver, which expresses highest levels of GAMT protein, served as a positive tissue control [54]. In Fig. 3a, every *mdx* muscle group revealed at least a 2.5-fold higher GAMT protein vs. C57. The top half of the blots were immunoblotted with desmin antibody to verify equal protein loading

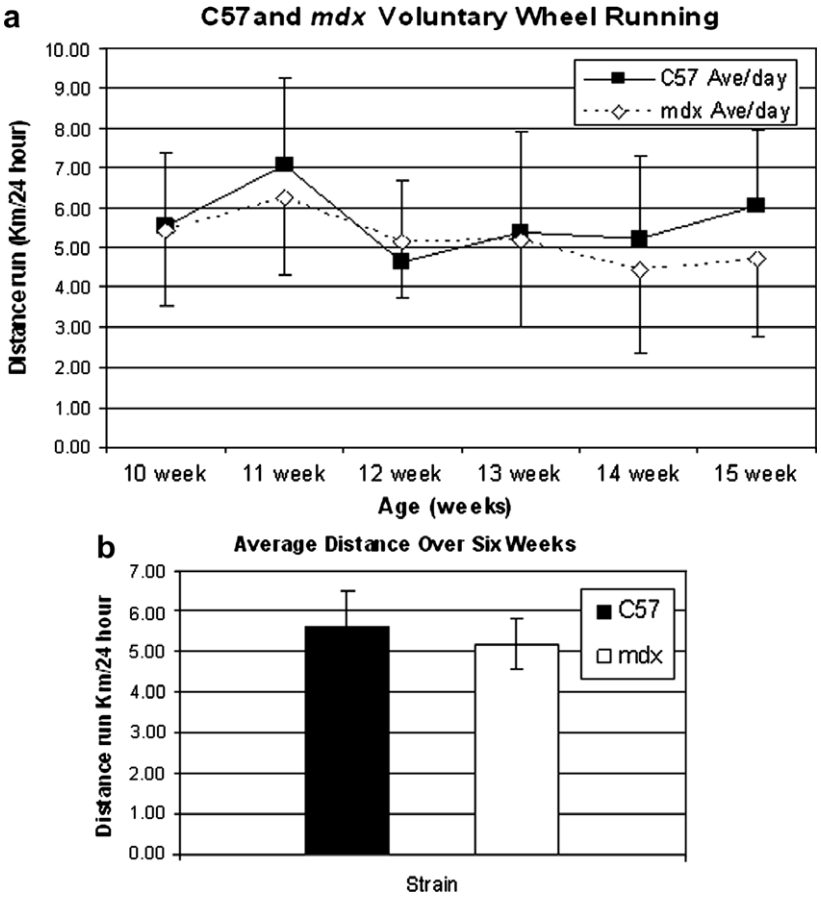

Fig. 1. Average distances run in a 24 h period were measured over a six week interval. In (a) C57 mice ($n = 10$) are denoted with a solid black box and *mdx* mice ($n = 12$) are denoted with an open diamond. In (b) bar graph summarizes the average daily voluntary wheel run distances of mature *mdx* and C57 mice. No statistical difference is seen.

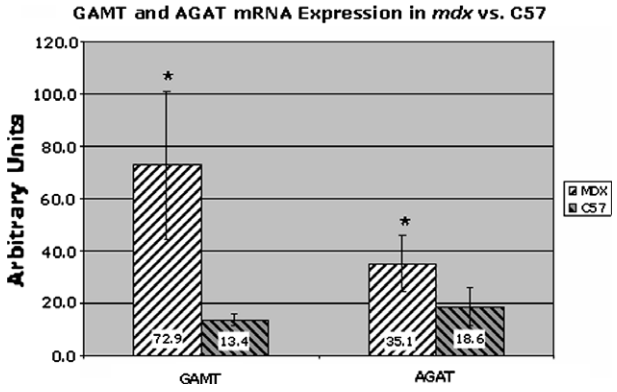

Fig. 2. Quantitative real time Taq-man RT-PCR in gastrocnemius muscles of 16 week old *mdx* vs C57 mice. In *mdx*, both GAMT and AGAT mRNAs are significantly elevated, with $p = 0.003$ and $p = 0.047$, respectively. *mdx* Mice ($n = 5$) are denoted by black and white diagonal bars while C57 ($n = 5$) are denoted by black and gray diagonal bars.

and internal expression controls (RF and TA blots are shown in Fig. 3b). Additional gels were run and stained with Coomassie blue to also verify equivalent loading of total protein in the gastrocnemius muscle (data not shown).

In Fig. 3c with western blot analysis of skeletal muscle, we show that 2 week and 4 week old C57 mice have elevated levels of GAMT signal which gradually decreases by 5 weeks of age and becomes undetectable by 16 weeks of age (Fig. 3a).

In contrast, 2 week, 4 week and 5 week old *mdx* mice have increased levels of GAMT immunoreactivity (Fig. 3c), which continued to show elevated levels through at least 16 weeks of age (Fig. 3a).

3.4. Creatine concentration

Creatine concentrations were determined in serum and homogenates of five different muscles. No statistically significant difference was found comparing control vs. *mdx* although there was a trend toward higher total serum creatine in *mdx* vs. control mouse serum (Table 1). Concentrations in both serum and muscle homogenates were comparable to levels previously reported in mouse [58].

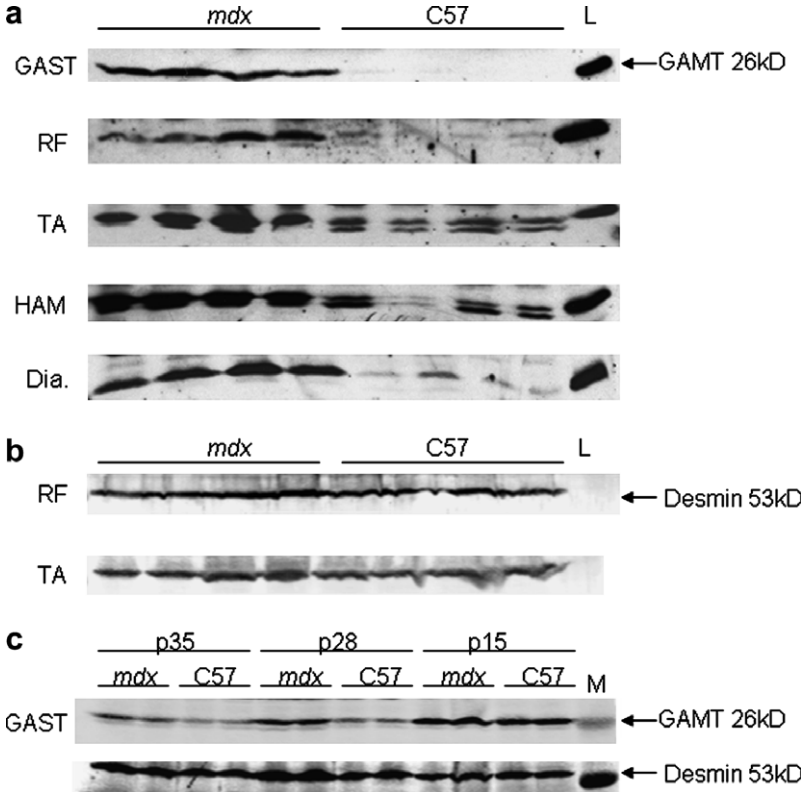

Fig. 3. (a) shows GAMT immunoblot analysis of five different muscle groups of 16 week old *mdx* and C57 mice. Lanes 1–4 are *mdx* and lanes 5–8 are C57. Lane 9 is liver used as a positive control tissue for GAMT protein. GAMT protein has a calculated $M_w = 26$ kDa. GAST is gastrocnemius; RF is rectus femoris; TA is tibialis anterior; HAM is hamstring; and Dia is diaphragm. $N = 8$–12 in all groups have been tested with this representative blot showing $n = 4$ per group. Two GAMT bands seen in the TA and HAM of C57 have unclear significance. Two alternative transcripts been reported in NCBI database and a human case report from lymphoblastoid tissue suggested the smaller GAMT species lacks a terminal exon and may be non-enzymatic [79]. The predominate GAMT band in the *mdx* mice is the larger 26 kDa species. The function of this smaller GAMT species in C57 is not known but does not undermine the observation that the *mdx* mouse highly upregulates 26 kDa GAMT unlike C57. (b) shows the upper half of blot membrane in (A) probed with desmin antibody to verify relative equal loading and internal expression control. Expected molecular weight of desmi $n = 53$ kDa. (c) Gastrocnemius immunoblot analysis for GAMT in mdx and C57 mice ages postnatal age 5 weeks, 4 weeks and 2 weeks. Desmin immunoblotting demonstrated equivalent protein loading and internal expression control for each sample.

Table 1
Creatine concentration in C57 vs *mdx* muscle and serum

	Serum	Gast	Ham	TA	RF	Diaph
C57	84.5 ± 49.2	86.5 ± 20.9	80.7 ± 29.7	21.9 ± 7.0	75.4 ± 21.1	50.6 ± 9.3
mdx	123.0 ± 39.4	96.8 ± 33.3	85.9 ± 30.0	31.9 ± 8.5	88.0 ± 57.1	50.2 ± 12.9

Serum creatine concentration (μM) is not statistically different in WT vs. *mdx* ($p = 0.1$).
n = 5–7.

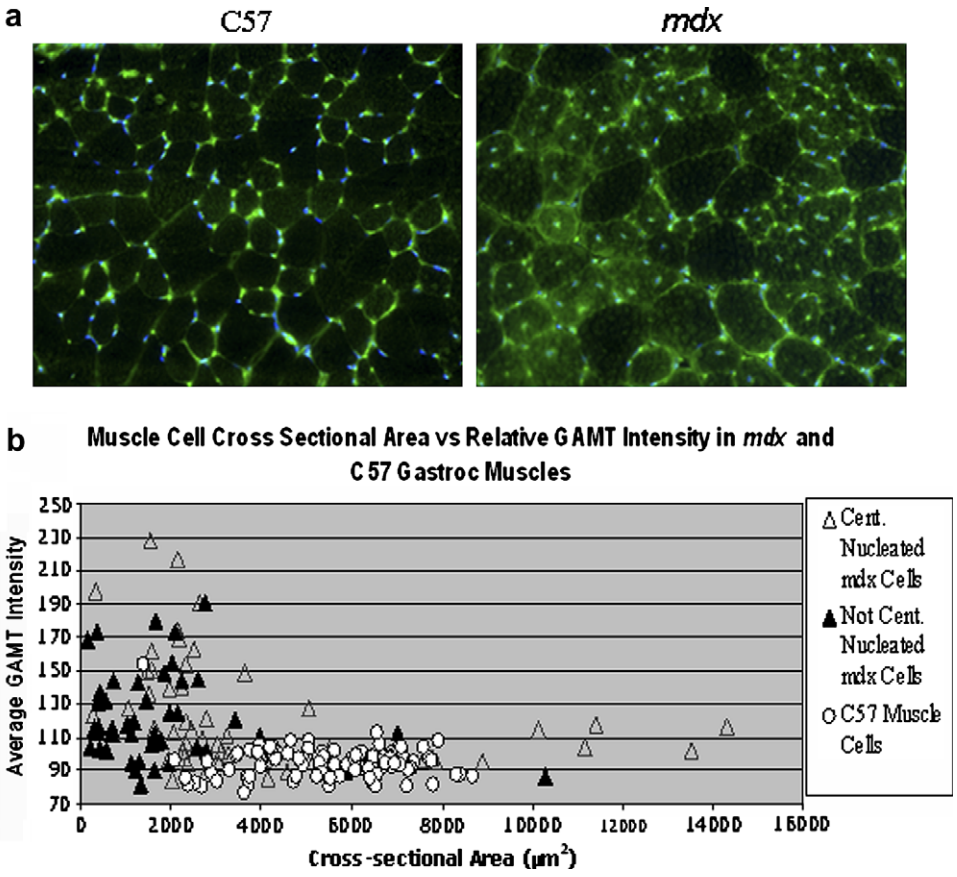

Fig. 4. (a) Indirect immunofluorescence of GAMT expression in transverse gastrocnemius cryosections of C57 and *mdx* mice. Sections were treated identically on the same slide and images were captured using identical exposure parameters. (b) Fiber cross-sectional area plotted against relative GAMT expression in 100 fibers of each C57 (○) and *mdx* gastrocnemius fibers grouped into central (▲) or non-central nucleated fibers (△).

3.5. Indirect immunofluorescence

GAMT protein cellular localization was performed using *in-situ* indirect immunofluorescence. Increased anti-GAMT immunofluorescence (green) in the gastrocnemius muscle was visualized in the cytoplasm in the majority (up to 80%) of muscle fibers of *mdx* mice while only background levels were seen in all fibers of control muscles (Fig. 4a). Dystrophin immunofluorescence (data not shown) revealed <3% revertant fibers which is consistent with previous reports [12]. The great majority of GAMT expression + fibers are visualized in widespread distribution far beyond the rare revertant fibers.

Single fiber characteristics were further investigated by performing more detailed image analysis. In Fig. 4b, single muscle fiber cross-sectional area was plotted against GAMT fluorescence intensity for 300 fibers. The *mdx* fibers were further grouped into central or non-central nucleated fibers, both of which can express high levels of GAMT protein. Control fibers have a much smaller range of fiber sizes ranging mostly from 3000 to 7000 μm^2 while *mdx* fibers range in size from 500 to 14,000 μm^2. Further analysis shows that control fibers (independent of size) have background levels of GAMT immunofluorescence, whereas the *mdx* fibers show higher immunofluorescence in all

fiber sizes with the greatest intensity being in the smaller caliber fibers with central nuclei (<2000 μm^2). Marked GAMT immunofluorescence intensity is also found in many of the mid-size (3000–7000 μm^2) *mdx* myofibers, which should be considered mature fibers when compared to control fibers of the same size Fig. 4a [59].

To determine if fibers expressing GAMT are only restricted to small regenerated fibers, anti-Embryonic Myosin Heavy Chain (EMyHC) was utilized on serial sections of gastrocnemeus muscles. Pathologic areas with degeneration–regeneration features are seen in mature *mdx* mice and a great majority of GAMT immunofluorescence is seen in non-pathologic areas. There are small fibers with both elevated GAMT levels and EMyHC+ immunolabelling in these pathologic areas and comprise less than 5% of total fibers (Fig. 5a). However, GAMT+ expression is not restricted to nascent small fibers that express EMyHC as GAMT immunofluorescence is observed in a greater majority of larger fibers that do not co-label with EMyHC (Fig. 5b).

In an effort to eliminate the possibility that *mdx* muscle fibers are prone to non-specific immunolabelling because of pathologic/inflammatory features, anti-GFP antibody was incubated with serial sections and showed no affinity to the sections (Fig. 5c). Finally sections were also incubated without primary antibody followed by secondary antibody to look for non-specific binding showing little to no background fluorescence (Fig. 5d).

Sixteen-week-old C57 gastrocnemius cryosections did not reveal immunoreactivity to GAMT nor EMyHC antibodies above background levels; nor with secondary antibody alone (data not shown).

3.6. Evans blue dye

Finally, we assessed the co-localization of GAMT immunofluorescence with Evans Blue Dye (EBD), a vital dye for identifying leaky cells, on triple-stained cryosections, (GAMT, green; EBD, red; & Hoechst, blue) (Fig. 6). Serial sections of a rare hyper-contracted fiber from mature *mdx* RF of the quadriceps muscle group are shown (40× objective lens). A loss of GAMT

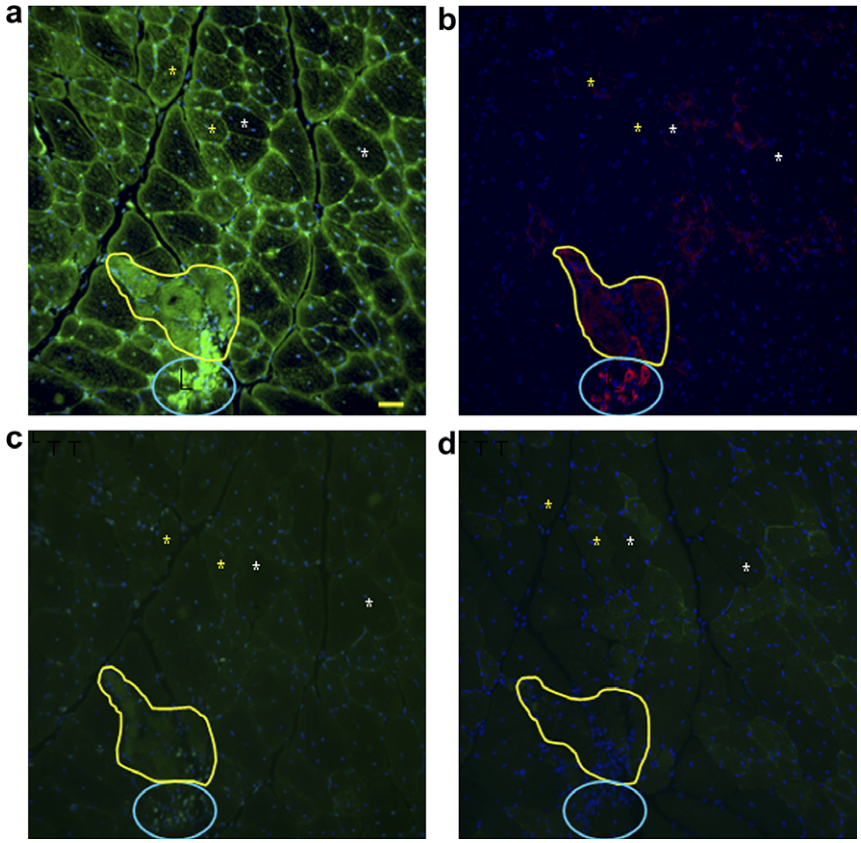

Fig. 5. Indirect immunofluorescence on serial cryosections to show both GAMT and EMyHC protein expression in gastrocnemius muscles of 16 weeks old *mdx* mice. (a) Muscle section immunostained for GAMT (green). The area within the yellow line is a pathologic region. (b) A serial section of (a), which shows the same region with fibers staining for EMyHC in red, circled with blue. Yellow stars denote fibers that are positive for GAMT and negative for EMyHC. White Xs denote fibers of a similar size that are negative for both GAMT and EMyHC. Adjacent cryosections incubated with a polyclonal antibody against green fluorescent protein in (c) for non-specific antigenicity labeling and (d) for secondary antibody only control for non-specific labeling. Sixteen-week-old C57 gastrocnemius cryosections are not immunoreactive to GAMT nor EMyHC antibodies (data not shown). Bar = 50 microns.

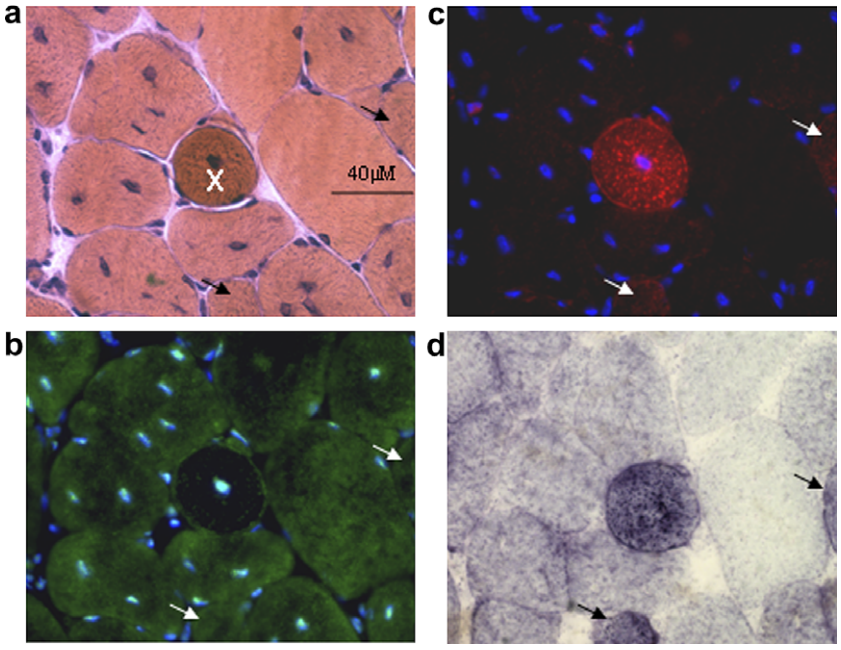

Fig. 6. (a–d) Serial sections showing an isolated hyper-contracted (pathologic) fiber, denoted with an X, from mature *mdx* rectus femoris. (a) H&E staining. Bar = 40 microns. (b) Indirect immunoflourescence of GAMT protein appears green with Alexa 488 plus nuclear DNA (blue) with Hoechst stain. (c) The same section as (b) using different filter set to show Evans Blue Dye (red) is leaking into a subset of cells. (d) shows succinate dehydrogenase (SDH) enzymatic activity with the greatest activity in the darkest fibers. White and black arrows denote fibers that are leaking (EBD positive), expressing GAMT, have high SDH activity but do not appear pathologic on H&E features. Images were captured using a 40× objective lens.

immunofluorescence (Fig. 6b) corresponds to the fiber of interest (X) shown in the H&E stain from (Fig. 6a). (Fig. 6c) shows presence of EBD (red) in the same fiber signifying membrane leakage. DNA in nuclei are stained with Hoechst (blue). This fiber is also highly oxidative as determined by succinate dehydrogenase (SDH) activity visible as dark blue. Some EBD+ fibers are also GAMT positive but these fibers did not necessarily appear pathologic (arrows). The great majority of *mdx* fibers with elevated GAMT immunofluorescence were not found to be hyper-contracted or severely damaged (H&E criteria) and the few pathologic fibers (hyalinized or hypercontracted) that were identified exhibited minimal to no GAMT immunofluorescence. Central nuclei are a pathologic but relatively minor feature compared to this hypercontracted basophilic appearance. We have seen at least ten severely pathologic fibers with these same features of EBD+, SDH+ and GAMT negative. Other *mdx* fibers that exhibited minimal GAMT immunofluorescence were the largest fibers ($<$7000 μm^2) in cross-section (Fig. 4) and tended to show traces of EBD uptake/fluorescence.

4. Discussion

Previous metabolic studies in *mdx* mouse skeletal muscle have revealed reductions in glycolytic and oxidative enzyme activities [60,61]. Similarly human DMD studies have reported reductions in glycolytic, glycogenolysis and oxidative enzymes [62–64]. However, one *mdx* study suggested that there may be discrete metabolic adaptations occurring in the phosphocreatine synthetic energy pathway through up-regulation of creatine kinase enzyme activity and protein content [49]. Nuclear magnetic resonance (NMR) studies [65,66] and a biochemical study [67] of *mdx* leg muscles have shown 80–90% of creatine in *mdx* vs control mice whereas NMR studies of boys with DMD showed only 20% of muscle creatine compared to controls [51] while urine creatine is 17-fold higher in boys with DMD vs. control [68].

Creatine in skeletal muscle acts to buffer the "cytosolic phosphorylation potential" for large fluctuations in energy demands. Creatine is not thought to be synthesized in skeletal muscle, but taken up from serum after synthesis in the liver or oral intake [48]. Therefore the aim of this study was to determine if there is an up-regulation of the creatine synthetic pathway in *mdx* skeletal muscle that could help maintain physiologic intracellular creatine concentrations despite leakage into the serum.

In adult control mice, tissue blots have previously shown GAMT protein is predominantly expressed in liver and testis, not skeletal muscle [54]. However, GAMT and AGAT protein are both found in the skeletal muscles of rat embryos and postnatal 21 day old control mice suggesting *de novo* creatine synthesis may have an important role in the development of embryonic

and perinatal skeletal muscle [58,69]. We believe that these features are also seen in small regenerative fibers (<500 μm^2) of adult *mdx* mice with the novel observation that GAMT and AGAT mRNA are both significantly higher in adult *mdx* vs. control muscles (Fig. 2). Fig. 3 shows that five different muscles have 2.5- to 5-fold greater GAMT protein immunoreactivity in adult *mdx* compared to control.

Fig. 3c demonstrates that GAMT protein expression is high in both *mdx* and control mice at 2 weeks of age. By 4 weeks and 5 weeks of age GAMT protein expression drops in both control and *mdx* mice, but *mdx* mice maintain higher GAMT protein levels from 4 weeks on and certainly at 16 weeks of age (Fig. 3a). GAMT immunofluorescence is detected in 80% of all skeletal fibers from the gastrocnemius in cross-section (Figs. 4a and 5a) while GAMT/AGAT mRNA levels are also upregulated (Fig. 2). It may be possible to reconcile the long-held mystery of why the *mdx* mouse appears to undergo a necrotic crisis phase exclusively at 3–6 weeks of age [5]. This decrease in GAMT expression could perhaps account for some aspect of this temporal relationship and recovery after 6 weeks of age. Other crisis factors may contribute including the following: weaning from nutrition of mother's breastmilk to standard rodent chow, increased weight-load, increased motor activity, etc.

These results suggest that *de novo* creatine synthesis can occur in small regenerating fibers but what about stably regenerated mature myofibers from adult *mdx*? To confirm that the mature fibers are not actively regenerating, serial sections of adult *mdx* muscle were stained for EMyHC and found that fewer than 5% of all fibers stained positive and were always of small caliber (<500 μm^2) as seen in Fig. 4b. Fibers that are EMyHC+ do indeed co-express GAMT at high levels, while other larger caliber mature fibers express marked GAMT without co-expression of EMyHC, as seen in Figs. 5a and b.

Considering the diaphragm has been shown to be the most severely affected muscle in *mdx* mice [11], one could postulate GAMT/AGAT would be decreased and not confer a compensatory role. However, we find the *mdx* diaphragm with western blot analysis shows an upregulation in GAMT protein. One explanation is different ages of *mdx* mice were studied (6 months vs. 4 months). This study investigated 4 month old (16 week old) *mdx* mice which do not have profound respiratory, exercise or histologic deficits while previous studies have shown severe pathologic alterations in the *mdx* diaphragm starting at 24 weeks of age (6 months) and histologically devastated by 16 month old *mdx* mice [12]. Another explanation may be that only small and/or regenerating fibers are expressing high levels of GAMT in the diaphragm while expression in the larger diaphragm fibers is not up regulated as seen in mature fibers of the hindlimb muscle groups (Fig. 5) but are shut down in the larger. Detailed single fiber diaphragm muscle immunolabelling analysis at different time points of mature and old mdx mice will be necessary to clarify this relationship if causal or incidental.

The up-regulation of GAMT protein expression in larger caliber (>2000 μm^2), *mdx* mature fibers can be seen in Figs. 4 and 5. Since half of the fibers ranging from 2000 to 7000 μm^2 express higher levels of GAMT protein (compared to C57), we believe GAMT plays more than just a development/regeneration role in the *mdx* muscle fibers. Increased GAMT may help maintain creatine concentration in *mdx* mature fibers making those fibers more resistant to the metabolic challenges of leaky membranes.

The difference in GAMT immunofluorescence between large and small caliber fibers may offer insights into regulation of GAMT expression that prove valuable in understanding its expression. The largest *mdx* fibers have very little GAMT immunoreactivity. If GAMT expression is important to limit energy failure and support muscle cell survival, this finding may offer an explanation to previous work that reports small caliber fibers do not suffer necrosis compared to larger fibers in *mdx* mice [70,71]. It seems that GAMT up-regulation in adult *mdx* skeletal muscle may support both regeneration requirements of nascent fibers and enhanced metabolic support of established mature fibers including many stably regenerated fibers with central nuclei. The data presented here demonstrates that AGAT/GAMT mRNA and GAMT protein are all upregulated in multiple skeletal muscles. We believe this strongly implicates the novel finding that *de novo* creatine synthesis can occur in skeletal muscles of mature *mdx* mouse. Substrate availability for this pathway however, has not been determined in this study. Dietary experiments are currently underway in which *mdx* mice are fed arginine and glycine supplemented diets.

In Fig. 7 we offer a model showing that *de novo* creatine synthetic upregulation in *mdx* mice could offer metabolic advantage for muscle cells which lack dystrophin and offset the sequelae of leaky membranes including metabolic compromises e.g. creatine kinase and creatine efflux. Maintaining normal ATP levels is essential for all normal muscle function including calcium pumps, myosin ATPases and membrane potentials. In addition to this model GAMT may have an important role in normal development and regeneration of skeletal muscle. We have begun studies breeding *mdx* mice with GAMT knockout mice. The GAMT null mice are small but viable and active [58]. Our double knockout studies should offer insights for possible GAMT loss-of-function effects. Initial observations of these double knockout mice have shown that they struggle to thrive prior to weaning (unpublished observations). Studies with

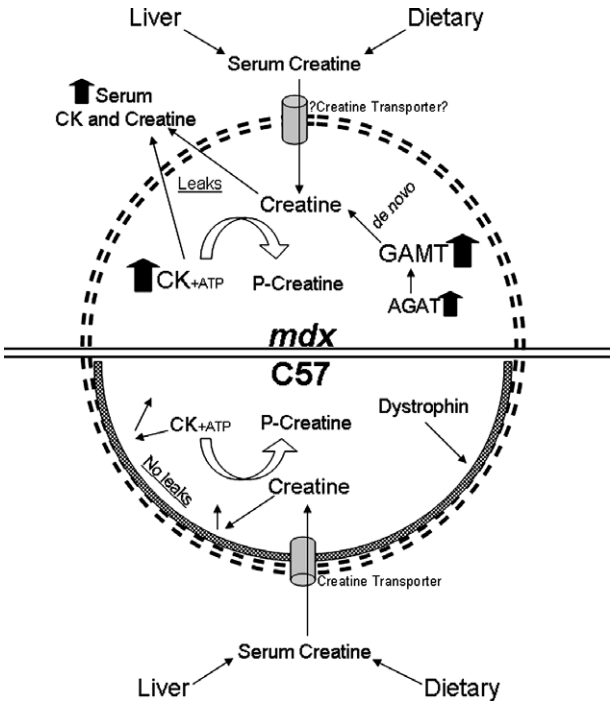

Fig. 7. We propose that leaky *mdx* muscle fibers are able to maintain near normal creatine concentrations by synthesizing creatine *de novo* through up-regulation of both GAMT and AGAT. The *de novo* synthesis of creatine would allow for discrete *mdx* metabolic adaptations to offset leaky membranes and excess loss of intracellular creatine. Limiting energy failure in muscle cells, *mdx* mice may be divergent in a unique metabolic adaptation compared to muscles from boys with DMD. Further studies including human analysis are warranted.

these mice should provide insight of the potential role of GAMT up-regulation and *de novo* creatine synthesis in skeletal muscles of mature *mdx* mice.

As the creatine synthetic pathway is being investigated in the *mdx* mouse, one may wonder why human DMD oral creatine supplementation studies have not found statistically significant benefit with functional activities, activities of daily living or modified manual muscle testing [72,73]. Supra-physiological levels of supplemental creatine (10–14% of diet from birth) resulted in no clear benefit in one *mdx* study [67], while a second oral creatine supplementation *mdx* study found histologic improvements in the EDL, not in the soleus [74]. We conclude oral creatine supplementation studies have not shown striking functional improvements in human DMD. It would be of value to further explore reasons for its limited benefits in DMD.

No direct study has ever demonstrated the existence of a functional creatine transporter (CrT) at the membrane of a dystrophin-deficient skeletal muscle, although it has been shown to localize on the membranes of control embryonic rat skeletal muscle in addition to brain and intestines [69]. Dystrophin-deficiency can lead to disrupted membrane complexes, such as those involving dystroglycans [75]. Freeze-fracture scanning electron-microscopy studies have shown a profound loss of intramembranous particle density in *mdx* skeletal muscles [76,77]. It stands to reason that transmembrane proteins and transporters such as the CrT may also have aberrant localization or impaired function in dystrophin-deficient muscles. Efficacy of oral creatine supplementation may be undermined if insufficient CrTs are at the muscle membranes of *mdx* and DMD. *Mdx* muscles maintain 80+% [67] (Table 1) of normal creatine levels. If *mdx* muscle cannot efficiently transport plasma creatine into the muscle cell compared to controls, one could deduce that *de novo* creatine synthesis in skeletal muscle with the increased GAMT expression would be advantageous. The downregulation of GAMT expression [45,63,78] coupled with an impaired CrT function may explain why human DMD muscle only contains 20% of normal creatine levels [51]. Detailed studies are warranted to characterize the localization and function of CrT in the *mdx* mouse and in humans with DMD.

The work described in this manuscript uncovers a novel facet to possibly explain why the *mdx* mouse is not crippled. We believe there are many differential genes and multiple compensatory mechanisms in the *mdx* mouse. This study adds a new aspect to that complex and evolving story. The work done here demonstrates discrete creatine synthesis capabilities in mature skeletal muscle fibers, not just small nascent fibers of the adult *mdx* mouse. Future promoter studies may help elucidate the apparent divergent signaling mechanisms that influence GAMT/AGAT gene regulation in mouse versus human skeletal muscle. In future efforts, these findings could be important directions to seek new targets and potential treatments for human DMD.

Acknowledgements

This work was supported by a grant from the National Institute of Arthritis and Musculoskeletal and Skin Diseases (ARϕ523ϕ8) to B.S.T. We thank Dr. Dirk Isbrandt (Hamburg, Germany) for his insights and rabbit anti-mouse GAMT polyclonal antibodies. We thank Dr. Brad Bendiak for critically reviewing this manuscript. We would like to acknowledge the DERC Molecular Core NIH P30 DK57516 for assistance with quantitative Real Time-PCR studies. We also thank John Van Hoven for assistance with insights, primer design and Reverse Transcription PCR and the University of Iowa Developmental Studies Hybridoma Bank for providing low cost EMyHC antibody. Research was supported by The Sharp Family and Hike for Hope Foundation, The Young Fund, The Children's Hospital Foundation, UCDHSC Departments of Pediatrics,

Neurology and Cell & Developmental Biology and NIH NIAMS K08 Mentored Clinician-Scientist Award.

References

[1] Koenig M, Hoffman EP, Bertelson CJ, Monaco AP, Feener C, Kunkel LM. Complete cloning of the Duchenne muscular dystrophy (DMD) cDNA and preliminary genomic organization of the DMD gene in normal and affected individuals. Cell 1987;50:509–17.

[2] Nonaka I. Animal models of muscular dystrophies. Lab Anim Sci 1998;48:8–17.

[3] Straub V, Rafael JA, Chamberlain JS, Campbell KP. Animal models for muscular dystrophy show different patterns of sarcolemmal disruption. J Cell Biol 1997;139:375–85.

[4] Watchko JF, O'Day TL, Hoffman EP. Functional characteristics of dystrophic skeletal muscle: insights from animal models. J Appl Physiol 2002;93:407–17.

[5] McArdle A, Edwards RH, Jackson MJ. Time course of changes in plasma membrane permeability in the dystrophin-deficient *mdx* mouse. Muscle Nerve 1994;17:1378–84.

[6] Reeve JL, McArdle A, Jackson MJ. Age-related changes in muscle calcium content in dystrophin-deficient *mdx* mice. Muscle Nerve 1997;20:357–60.

[7] Pastoret C, Sebille A. Time course study of the isometric contractile properties of *mdx* mouse striated muscles. J Muscle Res Cell Motil 1993;14:423–31.

[8] Sacco P, Jones DA, Dick JR, Vrbova G. Contractile properties and susceptibility to exercise-induced damage of normal and *mdx* mouse tibialis anterior muscle. Clin Sci (Lond) 1992;82:227–36.

[9] Carnwath JW, Shotton DM. Muscular dystrophy in the *mdx* mouse: histopathology of the soleus and extensor digitorum longus muscles. J Neurol Sci 1987;80:39–54.

[10] Coulton GR, Morgan JE, Partridge TA, Sloper JC. The *mdx* mouse skeletal muscle myopathy: I. A histological, morphometric and biochemical investigation. Neuropathol Appl Neurobiol 1988;14:53–70.

[11] Stedman HH, Sweeney HL, Shrager JB, et al. The *mdx* mouse diaphragm reproduces the degenerative changes of Duchenne muscular dystrophy. Nature 1991;352:536–9.

[12] Danko I, Chapman V, Wolff JA. The frequency of revertants in *mdx* mouse genetic models for Duchenne muscular dystrophy. Pediatr Res 1992;32:128–31.

[13] Wineinger MA, Abresch RT, Walsh SA, Carter GT. Effects of aging and voluntary exercise on the function of dystrophic muscle from *mdx* mice. Am J Phys Med Rehabil 1998;77:20–7.

[14] Carter GT, Wineinger MA, Walsh SA, Horasek SJ, Abresch RT, Fowler Jr WM. Effect of voluntary wheel-running exercise on muscles of the *mdx* mouse. Neuromuscul Disord 1995;5:323–32.

[15] Dupont-Versteegden EE, McCarter RJ, Katz MS. Voluntary exercise decreases progression of muscular dystrophy in diaphragm of *mdx* mice. J Appl Physiol 1994;77:1736–41.

[16] Hayes A, Williams DA. Beneficial effects of voluntary wheel running on the properties of dystrophic mouse muscle. J Appl Physiol 1996;80:670–9.

[17] Louboutin JP, Fichter-Gagnepain V, Thaon E, Fardeau M. Morphometric analysis of mdx diaphragm muscle fibres. Comparison with hindlimb muscles. Neuromuscul Disord 1993;3:463–9.

[18] Pastoret C, Sebille A. Further aspects of muscular dystrophy in *mdx* mice. Neuromuscul Disord 1993;3:471–5.

[19] Tidball JG, Wehling-Henricks M. Evolving therapeutic strategies for Duchenne muscular dystrophy: targeting downstream events. Pediatr Res 2004;56:831–41.

[20] Brussee V, Tardif F, Tremblay JP. Muscle fibers of *mdx* mice are more vulnerable to exercise than those of normal mice. Neuromuscul Disord 1997;7:487–92.

[21] Cullen MJ, Walsh J, Roberds SL, Campbell KP. Ultrastructural localization of adhalin, alpha-dystroglycan and merosin in normal and dystrophic muscle. Neuropathol Appl Neurobiol 1996;22:30–7.

[22] Iannaccone S, Quattrini A, Smirne S, et al. Connective tissue proliferation and growth factors in animal models of Duchenne muscular dystrophy. J Neurol Sci 1995;128:36–44.

[23] Porter JD, Khanna S, Kaminski HJ, et al. A chronic inflammatory response dominates the skeletal muscle molecular signature in dystrophin-deficient *mdx* mice. Hum Mol Genet 2002;11:263–72.

[24] Gilbert R, Nalbantoglu J, Petrof BJ, et al. Adenovirus-mediated utrophin gene transfer mitigates the dystrophic phenotype of *mdx* mouse muscles. Hum Gene Ther 1999;10:1299–310.

[25] Tinsley J, Deconinck N, Fisher R, et al. Expression of full-length utrophin prevents muscular dystrophy in *mdx* mice. Nat Med 1998;4:1441–4.

[26] Tinsley JM, Potter AC, Phelps SR, Fisher R, Trickett JI, Davies KE. Amelioration of the dystrophic phenotype of *mdx* mice using a truncated utrophin transgene. Nature 1996;384:349–53.

[27] Blake DJ, Weir A, Newey SE, Davies KE. Function and genetics of dystrophin and dystrophin-related proteins in muscle. Physiol Rev 2002;82:291–329.

[28] Bogdanovich S, Krag TO, Barton ER, et al. Functional improvement of dystrophic muscle by myostatin blockade. Nature 2002;420:418–21.

[29] Wagner KR, Liu X, Chang X, Allen RE. Muscle regeneration in the prolonged absence of myostatin. Proc Natl Acad Sci USA 2005;102:2519–24.

[30] Culligan K, Banville N, Dowling P, Ohlendieck K. Drastic reduction of calsequestrin-like proteins and impaired calcium binding in dystrophic *mdx* muscle. J Appl Physiol 2002;92:435–45.

[31] Doran P, Dowling P, Lohan J, McDonnell K, Poetsch S, Ohlendieck K. Subproteomics analysis of Ca^{+}-binding proteins demonstrates decreased calsequestrin expression in dystrophic mouse skeletal muscle. Eur J Biochem 2004;271:3943–52.

[32] Dowling P, Doran P, Ohlendieck K. Drastic reduction of sarcalumenin in Dp427 (dystrophin of 427 kDa)-deficient fibres indicates that abnormal calcium handling plays a key role in muscular dystrophy. Biochem J 2004;379:479–88.

[33] Anderson JEMurray L. Barr Award Lecture. Studies of the dynamics of skeletal muscle regeneration: the mouse came back! Biochem Cell Biol 1998;76:13–26.

[34] de Martinville B, Kunkel LM, Bruns G, et al. Localization of DNA sequences in region Xp21 of the human X chromosome: search for molecular markers close to the Duchenne muscular dystrophy locus. Am J Hum Genet 1985;37:235–49.

[35] DiMario J, Strohman RC. Satellite cells from dystrophic (mdx) mouse muscle are stimulated by fibroblast growth factor in vitro. Differentiation 1988;39:42–9.

[36] Kobinger GP, Louboutin JP, Barton ER, Sweeney HL, Wilson JM. Correction of the dystrophic phenotype by in vivo targeting of muscle progenitor cells. Hum Gene Ther 2003;14:1441–9.

[37] Morgan JE, Hoffman EP, Partridge TA. Normal myogenic cells from newborn mice restore normal histology to degenerating muscles of the *mdx* mouse. J Cell Biol 1990;111:2437–49.

[38] Sahashi K, Ibi T, Suoh H, et al. Immunostaining of dystrophin and utrophin in skeletal muscle of dystrophinopathies. Intern Med 1994;33:277–83.

[39] Taylor J, Muntoni F, Dubowitz V, Sewry CA. The abnormal expression of utrophin in Duchenne and Becker muscular dystrophy is age related. Neuropathol Appl Neurobiol 1997;23:399–405.

[40] Boer JM, de Meijer EJ, Mank EM, van Ommen GB, den Dunnen JT. Expression profiling in stably regenerating skeletal muscle of dystrophin-deficient *mdx* mice. Neuromuscul Disord 2002;12(Suppl 1):S118–24.
[41] Rouger K, Le Cunff M, Steenman M, et al. Global/temporal gene expression in diaphragm and hindlimb muscles of dystrophin-deficient (mdx) mice. Am J Physiol Cell Physiol 2002;283:C773–84.
[42] Tkatchenko AV, Le Cam G, Leger JJ, Dechesne CA. Large-scale analysis of differential gene expression in the hindlimb muscles and diaphragm of *mdx* mouse. Biochim Biophys Acta 2000;1500:17–30.
[43] Tseng BS, Zhao P, Pattison JS, et al. Regenerated *mdx* mouse skeletal muscle shows differential mRNA expression. J Appl Physiol 2002;93:537–45.
[44] Chen Y-W, Zhao P, Borup R, Hoffman EP. Expression profiling in the muscular dystrophies: identification of novel aspects of molecular pathophysiology. J Cell Bio 2000;151:1321–36.
[45] Haslett JN, Kunkel LM. Microarray analysis of normal and dystrophic skeletal muscle. Int J Dev Neurosci 2002;20:359–65.
[46] Noguchi STT, Fujita M, Kurokawa R, et al. cDNA microarray analysis of individual Duchenne muscular dystrophy patients. Hum Mol Genet 2003;12:595–600.
[47] Wyss M, Felber S, Skladal D, Koller A, Kremser C, Sperl W. The therapeutic potential of oral creatine supplementation in muscle disease. Med Hypotheses 1998;51:333–6.
[48] Wyss M, Kaddurah-Daouk R. Creatine and creatinine metabolism. Physiol Rev 2000;80:1107–213.
[49] Ge Y, Molloy MP, Chamberlain JS, Andrews PC. Proteomic analysis of mdx skeletal muscle: great reduction of adenylate kinase 1 expression and enzymatic activity. Proteomics 2003;3:1895–903.
[50] Dunn JF, Tracey I, Radda GK. Exercise metabolism in Duchenne muscular dystrophy: a biochemical and [31P]-nuclear magnetic resonance study of *mdx* mice. Proc Biol Sci 1993;251:201–6.
[51] Sharma U, Atri S, Sharma MC, Sarkar C, Jagannathan NR. Skeletal muscle metabolism in Duchenne muscular dystrophy (DMD): an in vitro proton NMR spectroscopy study. Magn Reson Imaging 2003;21:145–53.
[52] Kiernan JA. Histological & histochemical methods: theory and practice. 2nd ed. Oxford, England; New York: Pergamon Press; 1990.
[53] Zhao P, Caretti G, Mitchell S, et al. Fgfr4 is required for effective muscle regeneration in vivo. Delineation of a MyoD-Tead2-Fgfr4 transcriptional pathway. J Biol Chem 2006;281:429–38.
[54] Lee H, Ogawa H, Fujioka M, Gerton GL. Guanidinoacetate methyltransferase in the mouse: extensive expression in Sertoli cells of testis and in microvilli of caput epididymis. Biol Reprod 1994;50:152–62.
[55] Conn Jr RB. Fluorimetric determination of creatine. Clin Chem 1960;6:537–48.
[56] Webster C, Silberstein L, Hays AP, Blau HM. Fast muscle fibers are preferentially affected in Duchenne muscular dystrophy. Cell 1988;52:503–13.
[57] Ikeda Y, Martone M, Gu Y, et al. Altered membrane proteins and permeability correlate with cardiac dysfunction in cardiomyopathic hamsters. Am J Physiol Heart Circ Physiol 2000;278:H1362–70.
[58] Schmidt A, Marescau B, Boehm EA, et al. Severely altered guanidino compound levels, disturbed body weight homeostasis and impaired fertility in a mouse model of guanidinoacetate *N*-methyltransferase (GAMT) deficiency. Hum Mol Genet 2004;13:905–21.
[59] Roig M, Roma J, Fargas A, Munell F. Longitudinal pathologic study of the gastrocnemius muscle group in *mdx* mice. Acta Neuropathol (Berl) 2004;107:27–34.
[60] Kuznetsov AV, Winkler K, Wiedemann FR, von Bossanyi P, Dietzmann K, Kunz WS. Impaired mitochondrial oxidative phosphorylation in skeletal muscle of the dystrophin-deficient *mdx* mouse. Mol Cell Biochem 1998;183:87–96.
[61] Chinet AE, Even PC, Decrouy A. Dystrophin-dependent efficiency of metabolic pathways in mouse skeletal muscles. Experientia 1994;50:602–5.
[62] Chen YW, Nagaraju K, Bakay M, et al. Early onset of inflammation and later involvement of TGFbeta in Duchenne muscular dystrophy. Neurology 2005;65:826–34.
[63] Chen YW, Zhao P, Borup R, Hoffman EP. Expression profiling in the muscular dystrophies: identification of novel aspects of molecular pathophysiology. J Cell Biol 2000;151:1321–36.
[64] Chi MM, Hintz CS, McKee D, et al. Effect of Duchenne muscular dystrophy on enzymes of energy metabolism in individual muscle fibers. Metabolism 1987;36:761–7.
[65] Dunn JF, Tracey I, Radda GK. A 31P-NMR study of muscle exercise metabolism in *mdx* mice: evidence for abnormal pH regulation. J Neurol Sci 1992;113:108–13.
[66] McIntosh LM, Baker RE, Anderson JE. Magnetic resonance imaging of regenerating and dystrophic mouse muscle. Biochem Cell Biol 1998;76:532–41.
[67] Louis M, Raymackers JM, Debaix H, Lebacq J, Francaux M. Effect of creatine supplementation on skeletal muscle of *mdx* mice. Muscle Nerve 2004;29:687–92.
[68] Vanpilsum JF, Wolin EA. Guanidinium compounds in blood and urine of patients suffering from muscle disorders. J Lab Clin Med 1958;51:219–23.
[69] Braissant O, Henry H, Villard AM, Speer O, Wallimann T, Bachmann C. Creatine synthesis and transport during rat embryogenesis: spatiotemporal expression of AGAT, GAMT and CT1. BMC Dev Biol 2005;5:9.
[70] Karpati G, Carpenter S. Small-caliber skeletal muscle fibers do not suffer deleterious consequences of dystrophic gene expression. Am J Med Genet 1986;25:653–8.
[71] Karpati G, Carpenter S, Prescott S. Small-caliber skeletal muscle fibers do not suffer necrosis in *mdx* mouse dystrophy. Muscle Nerve 1988;11:795–803.
[72] Tarnopolsky MA, Mahoney DJ, Vajsar J, et al. Creatine monohydrate enhances strength and body composition in Duchenne muscular dystrophy. Neurology 2004;62:1771–7.
[73] Escolar DM, Buyse G, Henricson E, et al. CINRG randomized controlled trial of creatine and glutamine in Duchenne muscular dystrophy. Ann Neurol 2005;58:151–5.
[74] Passaquin AC, Renard M, Kay L, et al. Creatine supplementation reduces skeletal muscle degeneration and enhances mitochondrial function in *mdx* mice. Neuromuscul Disord 2002;12:174–82.
[75] Ohlendieck K, Campbell KP. Dystrophin-associated proteins are greatly reduced in skeletal muscle from *mdx* mice. J Cell Biol 1991;115:1685–94.
[76] Shibuya S, Wakayama Y, Murahashi M, et al. Muscle plasma membrane changes in dystrophin gene exon 52 knockout mouse. Pathol Res Pract 2001;197:441–7.
[77] Shibuya S, Wakayama Y, Oniki H. Reduced density of intramembranous particle clusters: freeze-fracture study of *mdx* mouse muscle plasma membrane. Med Electron Microsc 2003;36:59–65.
[78] Noguchi S, Tsukahara T, Fujita M, et al. cDNA microarray analysis of individual Duchenne muscular dystrophy patients. Hum Mol Genet 2003;12:595–600.
[79] Leuzzi V, Carducci C, Carducci C, et al. A mutation on exon 6 of guanidinoacetate methyltransferase (GAMT) gene supports a different function for isoform a and b of GAMT enzyme. Mol Genet Metab 2006;87:88–90.